

Three-body force effect on the properties of nuclear matter under the gap and continuous choices within the BHF approach^{*}

WANG Pei(王培)^{1,2,3} ZUO Wei(左维)^{1,4,5;1)}

¹ Institute of Modern Physics, Chinese Academy of Sciences, Lanzhou 730000, China

² School of Physical Science and Technology, Lanzhou University, Lanzhou 730000, China

³ Graduate of Chinese Academy of Sciences, Beijing 100049, China

⁴ Kavli Institute for Theoretical Physics China, Chinese Academy of Sciences, Beijing 100190, China

⁵ State Key Laboratory of Theoretical Physics, Institute of Theoretical Physics, Chinese Academy of Sciences, Beijing 100190, China

Abstract: We have calculated and compared the three-body force effects on the properties of nuclear matter under the gap and continuous choices for the self-consistent auxiliary potential within the Brueckner-Hartree-Fock approach by adopting the Argonne V_{18} and the Bonn B two-body potentials plus a microscopic three-body force (TBF). The TBF provides a strong repulsive effect on the equation of state of nuclear matter at high densities for both the gap and continuous choices. The saturation point turns out to be much closer to the empirical value when the continuous choice is adopted. In addition, the dependence of the calculated symmetry energy upon the choice of the self-consistent auxiliary potential is discussed.

Key words: nuclear matter, Brueckner-Hartree-Fock approach, three-body force, gap choice, continuous choice

PACS: 21.65.Cd, 21.60.De, 21.30.-x **DOI:** 10.1088/1674-1137/38/8/084102

1 Introduction

One of the original aims of the microscopic Bethe-Brueckner-Goldstone (BBG) theory of nuclear matter [1] is to study the equation of state (EoS) of nuclear matter and reconcile the empirical saturation point. There are two most important uncertain points in the BBG theory [1]. One is the choice of the auxiliary potential $U(k)$, another is the relevance of the higher order contributions in the BBG expansion. Over the last decades, the many-body uncertainties in the BBG theory have been checked carefully, and considerable progress has been made in improving the predicted saturation point.

In an early stage of the BBG theory [2–4], the auxiliary potential $U(k)$ was introduced based on the resummation of Feynman diagrams [3], in order to decrease the number of diagrams in the calculation [2, 4]. It has been argued that different choices for the self-consistent auxiliary potential affect the convergence rate of the hole-line expansion, and can produce energy shifts in the calculated total binding energy [5]. As shown by Day and Wiringa [6, 7], the three-hole line contribution in the BBG expansion is non-negligible in the gap choice of the auxiliary potential. Baldo and Song have extended

the analysis to symmetric nuclear matter [8–10] and pure neutron matter [11] at the three-hole line level with the local separable Argonne V_{14} (AV14) [12] and Argonne V_{18} (AV18) [13] two-nucleon potentials by solving the Bethe-Fadeev equations [2, 14]. Their results give strong evidence that convergence has been reached [15, 16] within the gap and continuous choices for density up to six times the saturation value [17]. Furthermore, the results show that using the continuous choice leads to a faster convergence than the gap choice [8]. Since the EoS of nuclear matter are obtained at the level of two-hole line, the results of Ref. [8] indicate that the Brueckner-Hartree-Fock (BHF) approximation under the continuous choice is able to incorporate most of the three-hole correlations within the gap choice. Although the convergence can be reached, the BHF approach is not able to reproduce the empirical saturation point by adopting purely two-body interactions in both the gap and the continuous choices [8, 9, 17, 18]. Three-body forces (TBFs) are required for describing reasonably the nuclear saturation properties [19–22].

In recent years, calculations in the BHF approach have been updated by incorporating consistent microscopic TBFs [18–21] constructed with realistic Bonn B

Received 9 October 2013

^{*} Supported by National Natural Science Foundation of China (11175219), 973 Program of China (2013CB834405) and Knowledge Innovation Project (KJCX2-EW-N01) of Chinese Academy of Sciences, China

1) E-mail: zuowei@impcas.ac.cn

©2014 Chinese Physical Society and the Institute of High Energy Physics of the Chinese Academy of Sciences and the Institute of Modern Physics of the Chinese Academy of Sciences and IOP Publishing Ltd

[23] and AV18 two-nucleon potentials as input. As shown in Refs. [21, 22], the saturation points can be improved by including the TBFs from $(0.34 \text{ fm}^{-3}, -22 \text{ MeV})$ to $(0.17 \text{ fm}^{-3}, -15.9 \text{ MeV})$ and from $(0.27 \text{ fm}^{-3}, -18.3 \text{ MeV})$ to $(0.2 \text{ fm}^{-3}, -15.1 \text{ MeV})$, for the Bonn B and AV18 potentials respectively, under the continuous choice.

In this work, we extend the previous results within the BHF approach in the gap and continuous choices by employing the Bonn B and AV18 potentials plus their corresponding self-consistent TBFs, respectively. We concentrate on the comparison between the TBF effects on the properties of nuclear matter obtained under the gap choice and the continuous choice. The symmetry energy within the two different choices for the self-consistent auxiliary potential is also investigated and discussed. In Section 2, we give a brief review of the BHF theory and the TBF model. The numerical results are presented and discussed in Section 3. Our conclusions are summarized in the last section.

2 Formalism

Our calculations are based on the microscopic BHF approach. The BHF description of nuclear matter is derived by a linked cluster of independent hole-line expansion. The starting point of this theory is the in-medium two-body Brueckner reaction matrix G , which is the solution of the Bethe-Goldstone equation:

$$G(\rho; \omega) = v + v \sum_{k_1 k_2} \frac{|k_1 k_2\rangle Q(k_1, k_2) \langle k_1 k_2|}{\omega - \epsilon(k_1) - \epsilon(k_2) + i\eta} G(\rho; \omega), \quad (1)$$

where v is the realistic nucleon-nucleon (NN) interaction, ω is the starting energy, and ρ denotes nucleon number density. $Q(k_1, k_2)$ is the Pauli operator, which prevents the two nucleons from being scattered into their respective Fermi-seas. The single-particle (s.p.) energy is given by: $\epsilon(k) = \frac{\hbar^2 k^2}{2m} + U(k)$, where $U(k)$ is the auxiliary s.p. potential. Within the framework of the BHF approximation, the convergence rate of the hole-line expansion depends on the specified choice of the auxiliary potential [1]. Two different choices have been usually adopted in the BHF calculations [1]: the continuous choice and the gap choice. Under the continuous choice, the auxiliary potential is given by:

$$U(k) = \text{Re} \sum_{k' \leq k_F} \langle k k' | G[\rho, \epsilon(k) + \epsilon(k')] | k k' \rangle_A, \quad (2)$$

where the subscript A denotes antisymmetrization of the matrix elements. For the gap choice, the auxiliary potential for the hole states ($k < k_F$) is calculated according to Eq. (2), while it is set to zero above the Fermi surface ($k > k_F$). There are also other possibilities for choosing the auxiliary potential, e.g. the model-space BHF

(MBHF) [24]. In this work, we will restrict the calculations to the gap and continuous choices.

For the realistic NN interaction, we adopt different realistic two-body interactions (i.e., the AV18 and the Bonn B potentials [23]) plus their corresponding microscopic TBFs, which are based on the meson exchange current approach [19–22]. In the OBEP approximation, π , ρ , σ , ω mesons are considered and the corresponding meson parameters (meson-nucleon couplings and form factors) in the TBF model are determined self-consistently with the two-body potentials. In the present calculation, the TBF is reduced to an equivalently effective two-body force by averaging over the third nucleon degree of freedom in a nuclear medium [19, 25–27]:

$$\bar{V}_{ij}(r) = \rho \int d^3 r_k \sum_{\sigma_k, \tau_k} [1 - g(r_{ik})]^2 [1 - g(r_{jk})]^2 V_{ijk}, \quad (3)$$

where $g(r)$ is the defect function which reflects the NN correlations in nuclear medium. Within the BHF approximation, the energy per nucleon is given by:

$$\frac{B}{A} = \frac{3}{5} \frac{k_F^2}{2m} + \frac{1}{2\rho} \text{Re} \sum_{k, k' \leq k_F} \langle k k' | G[\rho; \epsilon(k) + \epsilon(k')] | k k' \rangle_A.$$

3 Results and discussion

Figure 1 shows the self-consistent single particle (s.p.) potentials in symmetric nuclear matter at density $\rho = 0.17 \text{ fm}^{-3}$, obtained under the gap choice (BHFG) and the continuous choice (BHFC) respectively. For the continuous choice, it is seen that the s.p. potential is strongly attractive at low momenta and its attraction decreases monotonically as a function of momentum continuously through the Fermi surface. In the gap choice, the self-consistent s.p. potential is cut off for momenta k larger than k_F , and shows a big gap at the Fermi surface. It is clear from Fig. 1 that the s.p. potentials are more attractive in the continuous choice than those in the gap choice, indicating that the effective interaction is more strongly attractive between the nucleons in the continuous choice than the gap choice. This is consistent with the analysis in Refs.[5, 8, 28], where it has been shown that the suppression of the gap at k_F in the s.p. potential tends to increase the correlation energy.

The TBF effects on the s.p. potential are also reported in Fig. 1 (dashed lines) with the gap choice and the continuous choice, respectively. We find that the TBF leads to a repulsive contribution and affects the s.p. potential mainly in the low momentum region not only for the Bonn B potential (right panel) but also for the AV18 potential (left panel), besides the lower magnitude for the AV18 potential, both in the gap and the continuous choices. In addition, one may notice the discrepancy (about 3–4 MeV at $k=0 \text{ fm}^{-1}$) between the

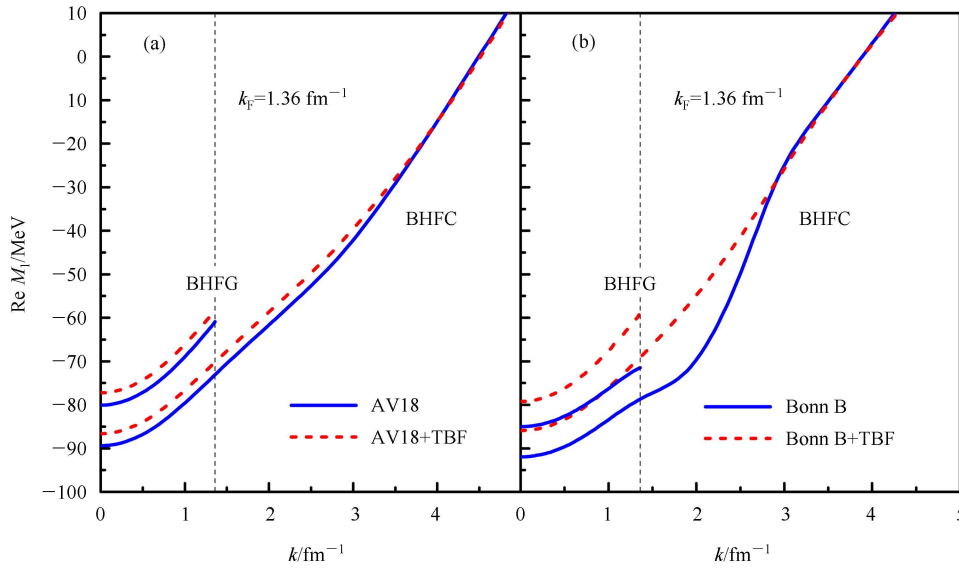


Fig. 1. (color online) (a) The s.p. potential in symmetric nuclear matter at $\rho=0.17 \text{ fm}^{-3}$, obtained with the AV18 potential. The dashed (red) curves have been obtained by taking into account the TBF contribution, while the solid (blue) curves denote the results without including the TBF. The vertical dashed lines show the location of the Fermi surface. The s.p. potentials discontinuous and continuous at the Fermi momentum k_F correspond to the gap (BHFG) and continuous choice (BHFC), respectively. (b) The same as in (a), but for the Bonn B potential.

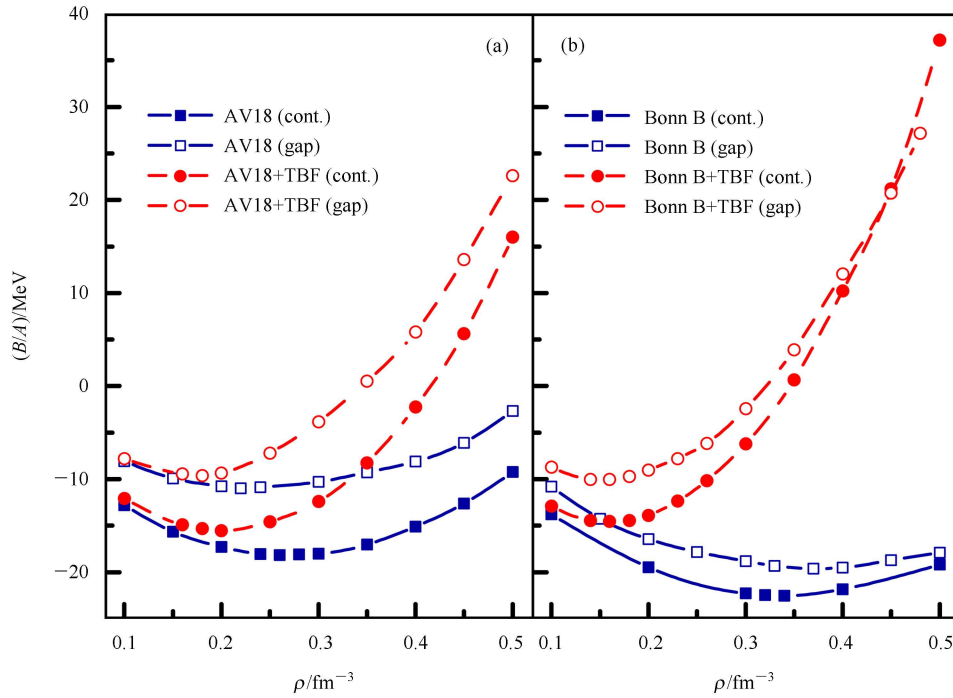


Fig. 2. (color online) (a) Energy per nucleon calculated for symmetric nuclear matter with the AV18 potential. The lines with circles have been obtained by taking into account the TBF contribution, while the square symbols denote the results without considering the TBF. Open and filled symbols correspond to the two cases with the gap and continuous choice for the auxiliary potential, respectively. (b) The same as in (a), but for the Bonn-B potential.

s.p. potentials obtained using the AV18 and Bonn B potentials. The discrepancy turns out to be regardless of the different choices for the auxiliary s.p. potential and can be traced back to the totally different analytical structures of the local potential (AV18) and the non-local potential (Bonn B). The non-locality in the Bonn B potential increases the attractive strength of the s.p. potential [29, 30].

In Fig. 2 the saturation curves are given as a function of density in symmetric nuclear matter with the gap and the continuous choices adopted. For the two-nucleon AV18 potential (left panel), the results are in good agreement with the previous two-hole line BHF calculation in Ref. [17], with the maximum deviation less than 1 MeV for density up to 0.5 fm^{-3} , both in the gap and the continuous choices. Under the continuous choice, the results of Fig. 2 have already been obtained in Refs. [21] and [22] for the AV18 and Bonn B potentials plus the corresponding TBFs. Here we repeat those results simply to discuss the influence of the different choices of the auxiliary potential. One may notice that using the continuous choice tends to give binding energies about 4–6 MeV larger than the gap choice, since the continuous choice incorporates more non-negligible correlation effects in the nuclear medium. This has been confirmed in Refs. [8–10, 15, 16] by solving the three-body Bethe-Faddeev equation with a series of separable potentials and the full AV14, AV18 two-body interactions. Similar results hold for the Bonn B potential (right panel), except that the obtained EoSs are more attractive due to the non-locality of the Bonn B potential [29, 30].

On the standard BHF level, by adopting purely the AV18 and Bonn B two-body potentials, one also obtains strong binding (solid curves in Fig. 2). For comparison, the TBF effects are also displayed in the same figure. The TBFs adopted are self-consistently determined by the AV18 and Bonn B two-body potentials, respectively, in Refs. [21, 22]. The TBF gives a repulsive contribution to the EoSs (dashed curves) both in the gap and the continuous choices. The TBF effect is fairly small at low densities. The repulsive contribution of the TBF increase rapidly as a function of density, which leads to a stiffer EoS and lower binding energies at the saturation point as compared with the results from using purely the two-body interactions, under both the gap and continuous choices.

The saturation points extracted from the previous results are reported in Fig. 3. Moreover, we give additional results with the AV14 potential in the same figure for the sake of comparison. The results can be roughly classified into four cases, i.e., including TBF and excluding TBF respectively under the two different kinds of choices (the gap choice and the continuous choice). By adopting purely the AV14, AV18, and Bonn B two-body

potentials, the predicted saturation points clearly miss the empirical saturation region under both the gap and continuous choices. The saturation densities and the saturation energies obtained within the continuous choice are shown to be much larger than the empirical values. Similar results are applicable for the gap choice, but the saturation energies calculated using the AV14 and the AV18 potentials are slightly less than the empirical value. The above results are consistent with the conclusion of the “Coester band” both in the gap choice [1, 31] and the continuous choice [1, 18]. After including the TBFs (with the AV14, AV18, and Bonn B potentials), the predicted saturation properties of symmetric nuclear matter are improved remarkably by the TBF repulsion, especially in the continuous choice. For the gap choice, the TBFs lead to a significant improvement of the saturation density, whereas the saturation energies turn out to be too small. It is clearly seen that, after including the TBFs in the calculation, the predicted saturation points turn to be much closer to the empirical one in the continuous choice than the gap choice.

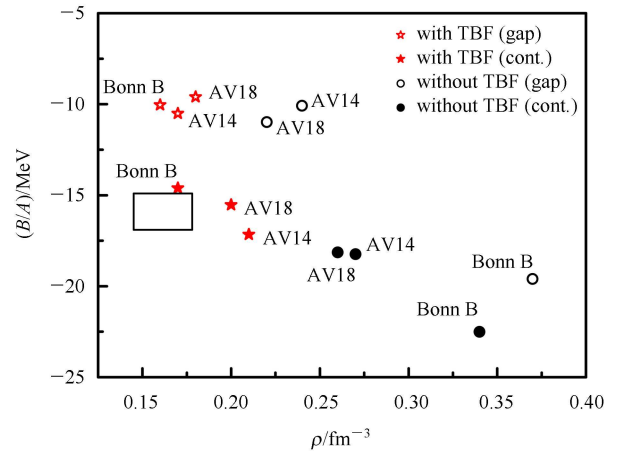


Fig. 3. (color online) Saturation points obtained by adopting different NN interactions under the gap and continuous choices for the auxiliary potential. The square indicates the empirical saturation region.

In Table 1, we compare the contributions from various partial wave channels to the potential energy of symmetric nuclear matter in the gap choice and the continuous choice at $\rho = 0.17 \text{ fm}^{-3}$. The S channel plays a dominant role, while the contributions from the P and D channels almost cancel each other out in the total potential energy when the AV18 and Bonn B two-body potentials plus their corresponding TBFs are adopted. A similar result has been reported in Ref. [5] by adopting the optical-model with the Reid hard core interaction. By comparing the results using the two different choices of the auxiliary s.p. potential, one may notice that the discrepancy between the total binding energies

Table 1. Potential energy per nucleon obtained for symmetric nuclear matter with the AV18 and Bonn B potentials in the gap and continuous choice, at $\rho=0.17 \text{ fm}^{-3}$. Units are given in MeV.

channel	AV18		AV18+TBF	
	gap	cont.	gap	cont.
1S_0	-15.87	-16.31	-13.05	-13.61
$^3S_1-^3D_1$	-15.86	-19.85	-16.82	-20.59
3P_0	-3.37	-3.44	-2.09	-2.11
3P_1	10.25	9.88	7.65	7.15
1P_1	3.95	3.87	3.34	3.28
1D_2	-2.67	-2.71	-2.05	-2.08
3D_2	-3.87	-3.97	-1.87	-1.88
$^3P_2-^3F_2$	-7.76	-8.15	-7.32	-7.76
$J \geq 3$	1.21	1.13	-0.39	-0.47
kinetic energy	23.04	23.04	23.04	23.04
total binding	-10.94	-16.5	-9.54	-15.03

Channel	Bonn B		Bonn B+TBF	
	Gap	Cont.	Gap	Cont.
1S_0	-16.67	-16.88	-14.65	-15.61
$^3S_1-^3D_1$	-17.3	-20.52	-18.52	-21.18
3P_0	-3.57	-3.61	-0.75	-0.34
3P_1	10.57	10.21	5.23	4.25
1P_1	1.52	2.36	4.01	3.45
1D_2	-2.43	-2.45	-0.93	-0.79
3D_2	-4.01	-4.1	-0.23	0.07
$^3P_2-^3F_2$	-7.89	-8.29	-6.48	-6.45
$J \geq 3$	1.84	1.74	-0.82	-1.04
kinetic energy	23.04	23.04	23.04	23.04
total binding	-14.92	-18.49	-10.1	-14.62

calculated in the gap and continuous choices mainly comes from the 3SD_1 channel, in fairly good agreement with the analysis in Ref. [10] using the AV14 potential. It is seen from Table 1 that, after including the TBF, the dominant effect of the $T=0$ SD coupled channel on the discrepancy remains the same as that obtained by adopting purely the AV18 and Bonn B two-body potentials.

In Fig. 4, the EoSs of pure neutron matter obtained within the gap and the continuous choices is reported. Due to lack of the strongly attractive effect of the tensor coupling in the isospin $T=0$ SD channel, a faster convergence of the hole-line expansion is expected for pure neutron matter than that for symmetric nuclear matter. It is seen that there is a weak dependence on the choice of the auxiliary s.p. potential using the AV18 and Bonn B two-body potentials (solid curves). The continuous choice tends to give slightly larger binding energies than the gap choice, with a maximum deviation of about 2 MeV, which is much less than that for symmetric nuclear matter (4–6 MeV). This result is in agreement with Ref. [11] and the smaller average depletion in the neutron Fermi sea [32]. After including the TBF, the convergence property remains the same as that obtained using purely the AV18 and Bonn B two-body potentials, whereas the EoSs become much stiffer at high densities.

According to the microscopic investigations [21, 33, 34], nuclear symmetry energy can be calculated as the difference between the energy per nucleon of pure

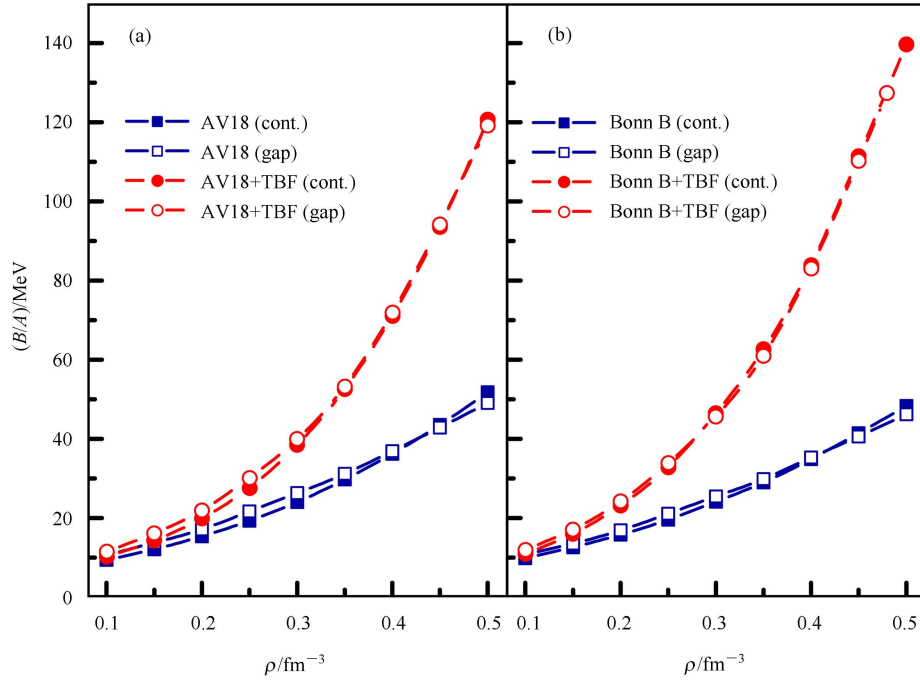


Fig. 4. (color online) The same as Fig. 2, but the results are obtained for pure neutron matter.

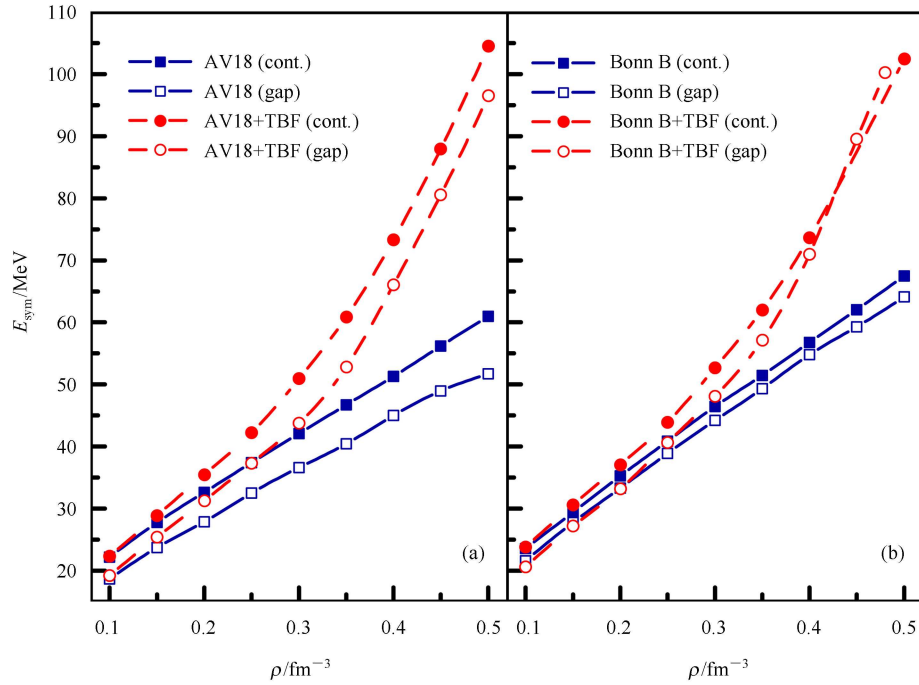


Fig. 5. (color online) (a) The symmetry energy obtained by adopting the AV18 two-body potential (blue curves with squares) and the AV18 potential plus the TBF (red curves with circles). Open and filled symbols correspond to the two cases with the gap and continuous choice for the auxiliary potential, respectively. (b) The same as in (a), but for the Bonn-B potential.

neutron matter and that of symmetric nuclear matter. Based on the results in Figs. 2 and 4, the symmetry energy is expected to depend on different choices of the auxiliary s.p. potential. Fig. 5 displays the symmetry energies obtained within the gap and the continuous choices, respectively. Under the continuous choice, the results in Fig. 5 have already been obtained and given in Refs. [21] and [35]. For all the cases presented in Fig. 5, the symmetry energy increases monotonically with increasing density, and becomes much stiffer at high densities when the TBF is self-consistently included in the calculation. The discrepancy between the calculated EoSs under the gap choice and the continuous choice, which is sizeable for symmetric matter, is substantially smaller for pure neutron matter. Consequently, the symmetry energy obtained under the gap choice turns out to be smaller than that under the continuous choice with both the AV18 and Bonn B two-body potentials. Similar results hold after including the TBFs. For the Bonn B potential, the discrepancy between the symmetry energies calculated in the gap choice and the continuous choice is quite small, especially at high densities.

4 Conclusions

We have studied and compared the TBF effects on the properties of symmetric nuclear matter and pure neu-

tron matter under the two different choices (i.e., the gap choice and the continuous choice) for the self-consistent auxiliary potential within the BHF approach. Special attention has been paid to discuss the difference between the TBF effects under the two different choices. In our calculation, the recent versions of the realistic AV18 and Bonn B two-body potentials plus the corresponding self-consistent microscopic TBFs have been employed. By adopting purely the two-body forces, symmetric nuclear matter turns out to be more binding under the continuous choice than that under the gap choice, confirming the previous results. Under both the gap and the continuous choices, the TBF effects on the EoSs of symmetric nuclear matter and pure neutron matter are repulsive. The repulsive TBF contribution increases rapidly as a function of density and leads to a significant improvement in the predicted nuclear saturation properties. Therefore, TBFs are necessary under both the gap and continuous choices for reliably predicting the EoS of nuclear matter and for reproducing the empirical saturation properties of nuclear matter within the framework of the BHF approach. Under the continuous choice, the saturation points calculated by including the TBF are closer to the empirical saturation point as compared with the predictions under the gap choice. After including the TBF, the convergence property remains the same as that for the two-body interactions. The TBF also affects considerably

the auxiliary s.p. potentials in the relatively low momentum region, making the s.p. potential less attractive. Furthermore, the symmetry energy obtained under the gap choice is shown to be slightly smaller than that under the continuous choice. Under both the gap and the continuous choices, the TBF plays an important role

in determining the high-density behavior of symmetry energy and its effect leads to a strong stiffening of symmetry energy at high densities.

In future, the TBF should be included at the three-hole line level for checking the convergency again by solving the Bethe-Fadeev equations.

References

- 1 Jeukenne J P, Lejeune A, Mahaux C. *Phy. Rep.*, 1976, **25**: 83
- 2 Brueckner K A, Gammel J L. *Phys. Rev.*, 1957, **105**: 1679; 1958, **109**: 1023
- 3 Kohler H S. *Nucl. Phys. A*, 1973, **204**: 65
- 4 Day B D. *Rev. Mod. Phys.*, 1967, **39**: 719
- 5 Jeukenne J P, Lejeune A, Mahaux C. *Phys. Rev. C*, 1974, **10**: 1391
- 6 Day B D. *Phys. Rev. C*, 1981, **31**: 1203
- 7 Day B D, Wiringa R B. *Phys. Rev. C*, 1985, **32**: 1057
- 8 Baldo M, Bombaci I, Giansiracusa G, Lombardo U. *J. Phys. G*, 1990, **16**: L263
- 9 Baldo M. *Nucl. Phys. A*, 1990, **519**: 243c
- 10 Baldo M, Bombaci I, Ferreira L S, Giansiracusa G, Lombardo U. *Phys. Rev. C*, 1991, **43**: 2605
- 11 Baldo M, Giansiracusa G, Lombardo U, SONG H Q. *Phys. Lett. B*, 2000, **473**: 1
- 12 Baldo M, Ferreira L S. *Phys. Lett. B*, 1991, **255**: 477
- 13 Wiringa R B, Stoks V G J, Schiavilla R. *Phys. Rev. C*, 1995, **51**: 38
- 14 Rajaraman R, Bethe H. *Rev. Mod. Phys.*, 1967, **39**: 745
- 15 SONG H Q, Baldo M, Giansiracusa G, Lombardo U. *Phys. Rev. Lett.*, 1998, **81**: 1584
- 16 SONG H Q, Baldo M, Giansiracusa G, Lombardo U. *Phys. Lett. B*, 1997, **411**: 237
- 17 Baldo M, Fiataro A, SONG H Q, Giansiracusa G, Lombardo U. *Phys. Rev. C*, 2001, **65**: 017303
- 18 Coon S A, Scadron M D, McNamee P C, Barrett B R, Blatt D W E, McKellar B H J. *Nucl. Phys. A*, 1979, **317**: 242; Ellis R G, Coon S A, McKellar B H J. *Nucl. Phys. A*, 1985, **438**: 631
- 19 Grangé P, Lejeune A, Martzolf M, Mathiot J F. *Phys. Rev. C*, 1989, **40**: 1040
- 20 ZUO W, Lejeune A, Lombardo U, Mathiot J F. *Nucl. Phys. A*, 2002, **706**: 418; *Eur. Phys. J. A*, 2002, **14**: 469
- 21 LI Z H, Lombardo U, Schulze H J, ZUO W. *Phys. Rev. C*, 2008, **77**: 034316
- 22 Machleidt R. *Adv. Nucl. Phys.*, 1989, **19**: 189; Brockmann R, Machleidt R. *Phys. Rev. C*, 1990, **42**: 1965
- 23 LI Z H, Lombardo U, Schulze H J, ZUO W, CHEN L W, MA H R. *Phys. Rev. C*, 2006, **74**: 047304
- 24 SONG H Q, Kuo T T S. *Phys. Rev. C*, 1991, **43**: 2883
- 25 ZHOU X R, Burgio G F, Lombardo U, Schulze H J, ZUO W. *Phys. Rev. C*, 2004, **69**: 018801
- 26 Baldo M, Ferreira L S. *Phys. Rev. C*, 1999, **59**: 682
- 27 Cheon T, Redish E F. *Phys. Rev. C*, 1989, **39**: 331; Sartor R. *Phys. Rev. C*, 1996, **54**: 809; Suzuki K, Okamoto R, Kohno M, Nagata S. *Nucl. Phys. A*, 2000, **665**: 92; Sammarruca F, MENG X, Stephenson E J. *Phys. Rev. C*, 2000, **62**: 014614
- 28 Bethe H A. *Annu. Rev. Nucl. Sci.*, 1971, **21**: 93
- 29 Baldo M, Maieron C. *Phys. Rev. C*, 2005, **72**: 034005
- 30 Muther H, Polls A. *Prog. Part. Nucl. Phys.*, 2000, **45**: 243
- 31 Coester F, Cohen S, Day B D, Vincent C M. *Phys. Rev. C*, 1970, **1**: 769
- 32 ZUO W, Lombardo U, Schulze H J. *Phys. Lett. B*, 1998, **432**: 241
- 33 Bombaci I, Lombardo U. *Phys. Rev. C*, 1991, **44**: 1892
- 34 ZUO W, Bombaci I, Lombardo U. *Phys. Rev. C*, 1999, **60**: 024605
- 35 LI Z H, Schulze H J. *Phys. Rev. C*, 2008, **78**: 028801